W. S. Godek. The authors would also like to acknowledge the support of the Materials Research Laboratory Program at Brown University and the helpful advice of Dr. A. Nozik of Allied Chemical Corp. and Dr. Kirby Dwight of Brown University.

Registry No. WO_3, 1314-35-8; KHF_2, 7789-29-9.

References and Notes

(1) A. Fujishima and K. Honda, *Nature (London)*, **238**, 37 (1972).
(2) A. J. Nozik, *Nature (London)*, **267** 383 (1975).
(3) For example J. G. Mavroides, D. I. Tcherneu, J. A. Kafalas, and D. F. Kolesar, *Mater. Res. Bull.*, **10**, 1023 (1975); M. S Wrighton, S. Grinley, P. T. Wolczanski, A. B. Ellis, D. L. Morse, and A. Linz, *Proc. Natl. Acad. Sci. U.S.A.*, **72**, 1518 (1975).
(4) J. G. Mavorides, J. A. Kafalas, and D. F. Kolesar, *Appl. Phys. Lett.*, **28**, 241 (1976).
(5) R. D. Nasby and R. K. Quinn, *Mater. Res. Bull.*, **11**, 985 (1976).
(6) K. L. Hardee and A. J. Bard, *J. Electrochem. Soc.*, **123**, 1024 (1976); R. K. Quinn, R. D. Nasby, and R. L. Baughman, *Mater. Res. Bull.*, **11**, 1011 (1976).
(7) H. Yoneyama, H. Sakamoto, and H. Tamura, *Electrochim. Acta*, **20**, 341 (1975).
(8) M. A. Butler, R. D. Nasby, and R. K. Quinn, *Solid State Commun.*, **19**, 1011 (1976).
(9) G. Hodes, D. Cahen, and J. Manassen, *Nature (London)*, **26**, 312 (1976).
(10) K. L. Hardee and A. J. Bard, *J. Electrochem. Soc.*, **124**, 215 (1977).
(11) D. M. Schleich, C. E. Derrington, W. Godek, D. Weisberg, and A. Wold, *Mater. Res. Bull.*, **12**, 331 (1977).
(12) L. J. van der Pauw, *Philips Tech. Rev.*, **20**, 220 (1958).
(13) G. Anderson, *Acta Chem. Scand.*, **7**, 154 (1953).
(14) S. Tanisaki, *J. Phys. Soc. Jpn.*, **15**, 566 (1960).
(15) P. Gado and A. Magnêli, *Acta, Chem. Scand.*, **19**, 1514 (1965).
(16) R. S. Roth and J. L. Waring, *J. Res. Natl. Bur. Stand., Sect. A*, **70**, 4, 281 (1966).
(17) E. Gebert and R. J. Ackermann, *Inorg. Chem.*, **5**, 136 (1966), and references cited therein.
(18) A. S. Ribnick, B. Post, and E. Banks, *Adv. Chem. Ser.*, **No. 39**, 246 (1963), and references cited therein.
(19) A. W. Sleight, *Inorg. Chem.*, **8**, 1764 (1969).
(20) T. G. Reynolds and A. Wold, *J. Solid State Chem.*, **6**, 565 (1973).
(21) S. K. Deb, *Philos. Mag.*, **27**, 801 (1973).
(22) W. Gissler and R. Memming, Electrochemical Society Virginia Conference, Airlie, Va., May 1977.

Contribution from the Department of Chemistry, University of Guelph, Guelph, Ontario, Canada, N1G 2W1,
Department of Chemistry, Leicester University, Leicester, LE1 7RH, England, Departêment de Chimie,
Institut Universitaire de Technologie de Rouen, 76130 Mont-Saint-Aignan, France,
and Bruker Spectrospin S.A., 67160 Wissembourg, France

Xenon-129 Pulse Fourier-Transform Nuclear Magnetic Resonance Spectroscopy

GARY J. SCHROBILGEN,*[1,2a,b] JOHN H. HOLLOWAY,[2b] PIERRE GRANGER,[2c] and CHRISTIAN BREVARD[2d]

Received October 21, 1977

High-resolution xenon-129 pulsed Fourier-transform NMR studies have been carried out on a variety of ^{129}Xe-containing compounds. New chemical shift data for this heavy nucleus in a wide range of oxidation states are summarized. The chemical shift range for ^{129}Xe in its compounds exceeds 4000 ppm which is consistent with large paramagnetic contributions to the shielding constant. In lieu of a comprehensive theory of heavy element chemical shifts, empirical correlations among ^{129}Xe chemical shifts are described which provide a sensitive probe for assessing the degree of ionic character in the Xe–F bond.

Introduction

Widespread interest in defining structures and properties of xenon fluorides and oxyfluorides, their cations, and related covalent species has resulted in several recent studies of their ^{19}F NMR spectra.[3-7] Among the naturally occurring isotopes of xenon, nuclear magnetic resonance spectroscopy of the nuclide ^{129}Xe ($I = {}^1/_2$, 26.2%) can, in principle, yield valuable complementary structural information. At the same time ^{129}Xe provides an ideal subject for a thorough investigation of a heavy nucleus since it can be obtained in a variety of compounds and in a wide range of oxidation states (+2, +4, +6, and +8).

A major difficulty in direct observation ^{129}Xe NMR spectroscopy has been the relatively low gyromagnetic ratio γ of ^{129}Xe, which yields a much smaller Boltzmann exponent, $2\gamma p_0 H/kT$, than that of fluorine. Xenon-129 resonance spectra are, therefore, weak and not easy to observe by conventional continuous-wave techniques. For this reason, early studies of the ^{129}Xe resonance have been confined to double-resonance "tickling" experiments in which one observes the effect on the ^{19}F spectrum of a small radio-frequency field swept through each line in the ^{129}Xe spectrum. These early experiments have yielded chemical shift values for $XeOF_4$, XeF_4, and XeF_2.[8,9] While the receptivity of natural-abundance ^{129}Xe is only 5.60×10^{-3} compared to the proton, natural-abundance ^{129}Xe possesses a receptivity that is 31.6 times that of natural-abundance ^{13}C, a nuclide now routinely studied by Fourier-transform techniques. Thus, the present availability of commercial pulse Fourier-transform spectrometers allows ready access to ^{129}Xe data which were previously unobtainable. Recent studies by direct observation F-T techniques have yielded new ^{129}Xe chemical shift data for XeF_4, XeF_6, XeO_3, $Xe(OSeF_5)_2$, $Xe(OTeF_5)_2$, $FXeOSeF_5$, $FXeOTeF_5$, and $F_5SeOXeOTeF_5$.[10,11] In the light of these developments it seemed timely to undertake an extensive study of all previously known and recently prepared xenon compounds. Preliminary results of our work have already been reported in a brief communication.[12]

The present state of understanding of chemical shifts of heavy nuclei is unclear. Our data, however, provide a substantial body of information on a single heavy nucleus, which can be used to probe the basis of these shifts. In lieu of a comprehensive theory of chemical shifts for heavy nuclei, our approach to the discussion of ^{129}Xe chemical shifts has remained essentially an empirical one. Where possible, however, attempts have been made to single out those factors which might play a dominant role in determining the observed trends. Thus, we have chosen to emphasize the very great sensitivity of the ^{129}Xe chemical shift to (1) formal oxidation state of xenon, (2) the ionic character of the Xe–F bond, and (3) solvent interactions. Structural elucidation of xenon species in solution by means of ^{129}Xe NMR has not been given great emphasis, as this aspect has already been adequately dealt with in a large number of instances using ^{19}F NMR spectroscopy. However, we have chosen to briefly discuss two examples in the light of the present ^{129}Xe NMR results which exhibit novel structural features, namely, the proposed tetramer $(XeF_6)_4$ and the recently reported xenon–nitrogen bonded compound $FXeN(SO_2F)_2$.

Discussion

Structures of Xenon Fluorides, Oxyfluorides, and Their Cations in Solution. Although the majority of the species

0020-1669/78/1317-0980$01.00/0

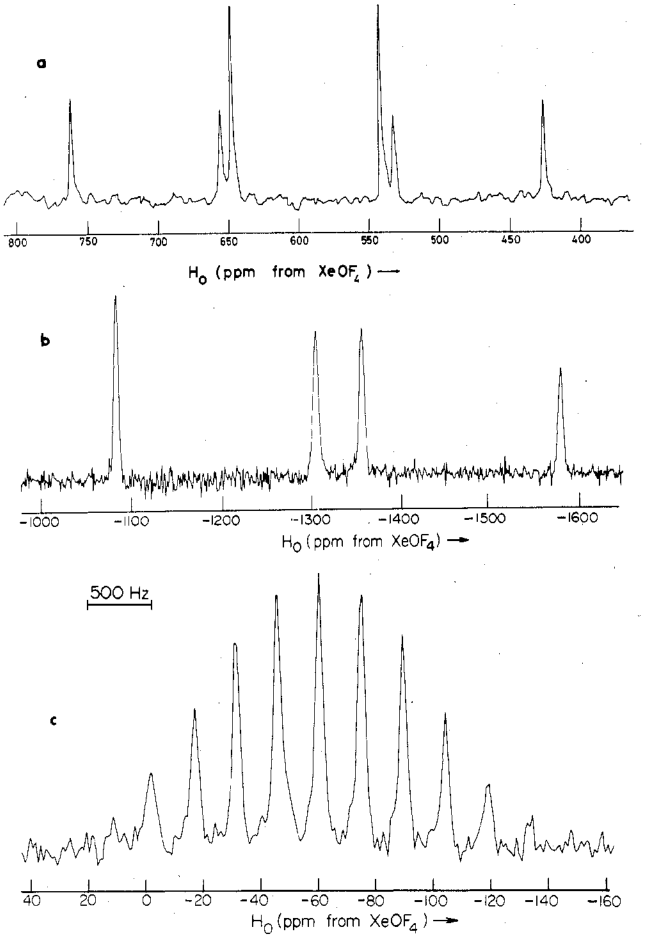

Figure 1. Xenon-129 NMR spectra of (a) the XeF_3^+ cation (0.76 *m* XeF_4 in SbF_5 solvent at 25 °C); (b) $FXeFWOF_4$ (0.86 *m* $XeF_2 \cdot WOF_4$ in BrF_5 solvent at -66 °C); (c) the XeF_6 tetramer (1.44 *m* XeF_6 in 50 mol % SO_2ClF/50 mol % CF_2Cl_2).

Table I. Comparison of Calculated and Experimental ^{129}Xe Chemical Shifts

	^{129}Xe chemical shift[a]		
Molecule	Calcd[b]	Exptl[c]	Exptl[d]
XeF_2	3420	3918	3930
XeF_6[e]	5500	5450	
$XeOF_4$	5750	5511	5511
XeF_4	5980	5764	5785

[a] $\delta_{^{129}Xe}$(atomic Xe) = 0 ppm. [b] Reference 19. [c] Direct observation of ^{129}Xe. [d] Determined from spin-tickling experiments in the ^{19}F NMR spectrum.[8,9] [e] The calculated value is for an octahedral XeF_6 monomer; the experimental value represents the chemical shift of XeF_6 tetramer.

reported in the present study have been characterized previously in solution by ^{19}F NMR,[3-7,13-15] a study of the ^{129}Xe resonance can be of value from the standpoint of gross structural considerations (Figure 1), especially when only one fluorine-on-xenon environment can be observed in the ^{19}F NMR spectrum. Thus, the observed fine structures arising from ^{19}F–^{129}Xe spin–spin coupling readily confirm the solution structures of such species as XeF^+, XeO_2F^+, XeO_2F_2, $XeOF_4$, $FXeSO_3F$, $(FXe)_2SO_3F^+$, and **1** (Table I).

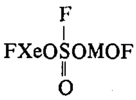
$$FXeO\overset{F}{\underset{O}{S}}OMOF_4$$

1, M = Mo or W

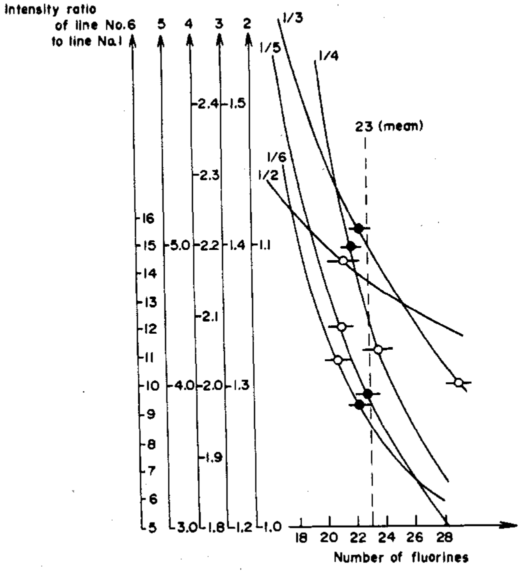

Figure 2. Graphical determination of *n* in $(XeF_6)_n$. Plots of outer line intensities:central line intensity for the ^{129}Xe NMR multiplet of $(XeF_6)_n$ vs. the total number of equivalent fluorines (6*n*) spin coupled to ^{129}Xe (● area by weighing, ○ peak height). The mean value of 6*n* determined graphically is 23 ± 2 or *n* = 4.

Xenon hexafluoride also exhibits a single ^{19}F environment in a 50 mol % SO_2ClF/50 mol % CF_2Cl_2 mixture at -145 °C. Using natural-abundance ^{129}Xe, a total of seven equally spaced lines having relative intensities of 0.1:2:15:60:100:60:15:2:0.1 and spacings of 115 Hz were observed. Upon enrichment to 60.1%, we were able to observe a total of nine lines of identical spacing having relative intensities of 3:18:50:85:100:85:50:18:3. The corresponding natural-abundance ^{129}Xe NMR spectrum of XeF_6 exhibits at least 11 equally spaced lines having spacings of 332 Hz (Figure 1c and Table II). The ^{19}F and ^{129}Xe NMR spectra of XeF_6 prepared from natural isotopic abundance xenon have been previously interpreted in terms of a polymeric species $(XeF_6)_n$, where *n* appears to be equal to 4.[11] We have also reinvestigated the ^{129}Xe NMR spectrum and have studied the intensity ratio between the central line (line 1) and the remaining outer lines of the ^{129}Xe NMR multiplet. A theoretical curve for each of the outer lines has been drawn in Figure 2 relating the number of equivalent spin–spin coupled fluorines to the intensity ratio (line 1:outer line). The experimental intensities have been measured by two methods, peak height and area by weighing. The measured intensity ratios have been plotted on the theoretical curves in order to obtain the total number of equivalent fluorines. The calculated mean value for 6*n*, 23 ± 2, corresponds to *n* = 4, confirming the earlier supposition that XeF_6 is tetrameric in solution at low temperatures. The detailed analysis of the ^{19}F NMR spectra and the mechanism for redistribution of all 24 fluorines over four chemically equivalent xenon atoms in $(XeF_6)_4$ are discussed in detail elsewhere.[16]

Le Blond and Des Marteau[15] have recently reported the synthesis of the first compound to contain xenon bonded to nitrogen, $FXeN(SO_2F)_2$. We have reinvestigated this novel system by means of ^{129}Xe NMR spectroscopy. In the course of our study, the ^{19}F NMR spectrum of $FXeN(SO_2F)_2$ was also recorded in BrF_5 in our laboratory and was found to be consistent with that reported by Le Blond and Des Marteau. The ^{19}F spectrum consists of two singlets with ^{129}Xe satellites at -57.6 ppm, $J_{^{129}Xe-^{19}F}$ = 18.7 Hz, and 126.1 ppm, $J_{^{129}Xe-^{19}F}$ = 5607 Hz. The low-field singlet is assigned to fluorine on sulfur and the high-field singlet to fluorine on xenon; the measured relative intensities were 2:1, respectively. We have also recorded the ^{129}Xe spectrum of the compound in BrF_5

Table II. Xenon-129 Nuclear Magnetic Resonance Parameters[a]

Species	$\delta_{^{129}Xe}$, ppm	$J_{^{129}Xe-^{19}F}$, Hz	Spin multiplicity[b]	Solute (molal concn)	Solvent	T, °C
Xe[c]	−5331		S	Xe	n-C_6F_{14}	25
$FXe(SO_2F)_2N$	−2016	~18 5572	T D	$FXe(SO_2F)_2N$ (~0.5)	BrF_5	−40
XeF_2	−1905	5630	T	XeF_2 (satd)	SO_2ClF	25
XeF_2	−1750	5616	T	XeF_2 (2.70)	BrF_5	25
XeF_2	−1708	5583	T	XeF_2 (2.70)	BrF_5	−40
$FXeOSO_2F$	−1467	5975	D	XeF_2 (2.81)	HSO_3F	−84
$Xe(OSO_2F)_2$	−1613		S			
$FXeOSO_2F$	−1416	6012	D	XeF_2 (2.81)	HSO_3F	−90
$Xe(OSO_2F)_2$	−1572		S			
XeF_2	−1592	5652	T	XeF_2 (~16)	HF	25
$FXeOSO_2F$	−1666	5830	D	$FXeSO_3F$ (1.20)	BrF_5	−40
$FXeOSO_2F$	−1613	5848	D	$FXeSO_3F$ (1.20)	BrF_5	−77
$FXeOSO_2F$	−1407	6051	D	$XeF_2 \cdot MoOF_4$ (1.32)	HSO_3F	−100
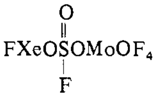 $FXeO\overset{O}{\underset{F}{S}}OMoOF_4$	−1342	5971	D			
$FXeOSO_2F$	−1416	ʻ6021	D	$XeF_2 \cdot WOF_4$ (1.00)	HSO_3F	−90
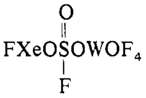 $FXeO\overset{O}{\underset{F}{S}}OWOF_4$	−1335	6131	D			
$FXeF \cdots MoOF_4$	−1383	5117 6139	D D	$XeF_2 \cdot MoOF_4$ (0.92)	BrF_5	−80
$FXeF \cdots WOF_4$	−1331	5051 6196	D D	$XeF_2 \cdot WOF_4$ (0.86)	BrF_5	−66
$FXeF \cdots MoOF_4$	−1441	5076 6058	D D	XeF_2 (0.98) $MoOF_4$ (2.13)	SO_2ClF	−118
$FXeF \cdots MoOF_4(MoOF_4)$	−1338	5036 6159	D D			
$FXeF \cdots MoOF_4(MoOF_4)_2$	−1321	5029 6156	D D			
$FXeF \cdots WOF_4$	−1315	5000 6127	D D	$XeF_2 \cdot 2WOF_4$ (0.70)	SO_2ClF	−115
$FXeF \cdots WOF_4(WOF_4)$	−1189	4964 6268	D D			
$FXeF \cdots WOF_4(WOF_4)_2$	−1170	4996 6304	D D			
$FXeOWF_5(WOF_4)$	−955	6373	D			
$FXeOWF_5(WOF_4)_2$	−906	6373	D			
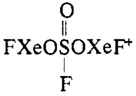 $FXeO\overset{O}{\underset{F}{S}}OXeF^+$	−1258	6428	D	$(FXe)_2SO_3F^+AsF_6^-$ (1.00)	BrF_5	−77
$FXe \cdots F \cdots XeF^+$	−1051	4865 6740	D D	$(FXe)_2F^+AsF_6^-$ (1.14)	BrF_5	−57
XeF^+	−574	7594	D	XeF_2 (0.71)	SbF_5	25
$(XeF_6)_4$	−60.8	331.7	–[d]	XeF_6 (1.44)	SO_2ClF/CF_2Cl_2[e]	−145
XeF_5^+	−23.9	165 1377	Q D	F_5XeSO_3F (1.32)	HSO_3F	−80
$XeOF_4$	0	1123	Q	$XeOF_4$ (4.48)	neat	25
$XeOF_4$	−0.1	1127	Q	$XeOF_4$ (~0.5)	SO_2ClF/CF_2Cl_2[e]	−145
XeF_5^+	12.7	159 1400	Q D	$XeF_5^+Sb_2F_{11}^-$(~4)	HF	25
XeO_2F_2	173.2	1217	T	XeO_2F_2 (~0.5)	HF	25
XeO_3[c]	217		S	XeO_3	H_2O	25
$XeOF_3^+$	238	434 1018	T D	$XeOF_3^+SbF_6^-$ (0.21)	SbF_5	25
XeF_4	253	3823	Q	XeF_4 (satd)	BrF_5	25
XeF_3^+	595	2384 2609	D T	XeF_4 (0.76)	SbF_5	25
XeO_2F^+	600	95	D	$XeO_2F^+SbF_6^-$ (satd)	SbF_5	25
XeO_6^{4-}	2077		S	Na_4XeO_6 (~0.5)	H_2O	25

[a] Spectra were recorded at 22.63 MHz in Fourier-transform mode and were referenced with respect to external $XeOF_4$ at 25 °C. [b] Key: S = singlet, D = doublet, T = triplet, and Q = quintet. [c] Reference 10. [d] Only 11 or the theoretical 25 lines in this spectrum have been observed (see Figure 1c). [e] 50 mol % SO_2ClF/50 mol % CF_2Cl_2.

solvent (Table I). The spectrum consists of a doublet (5572 Hz) of triplets (~18 Hz); the doublet arises from fluorine coupling of a single terminal ^{19}F to ^{129}Xe while the small triplet fine structure is indicative of a long-range spin–spin coupling between xenon and two equivalent fluorines on sulfur. Alternatively, we propose that the ^{129}Xe and ^{19}F data are also consistent with the oxygen-bonded structures Ia–c, in which the Xe–F group can be regarded as fluxional on the NMR time scale, exchanging over all four oxygens, giving rise to two equivalent fluorines on sulfur. On the basis of the demon-

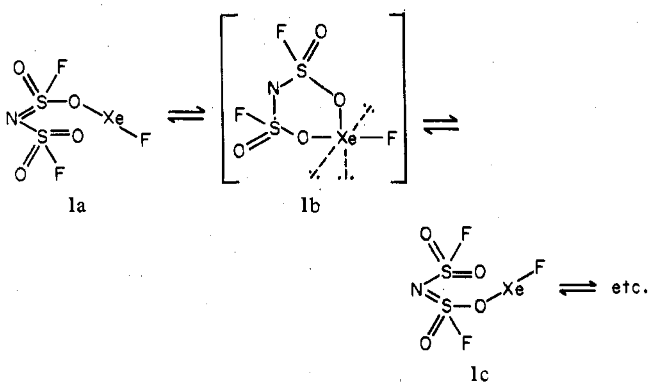

1a 1b 1c

strated empirical correlation between ^{19}F and ^{129}Xe chemical shifts described later in this work (Figure 3), it appears that the Xe–F group in $FXeN(SO_2F)_2$ may be oxygen bonded and not nitrogen bonded as previously supposed.

Choice of NMR Solvents. A thorough discussion of ^{129}Xe chemical shifts, which are sensitive to solvent composition, and related trends is complicated by the fact that it is not possible to study the majority of xenon species in a common solvent. The selection of suitable solvents in these studies is limited not only by straightforward solubility considerations but also by solvent–solute reactions, i.e., by (1) the relative fluoride donor–acceptor properties of the solute and the solvent and by (2) the resistance of the solvent to oxidation by a particular oxidation state of xenon.

In all cases, the xenon fluoro—and oxyfluoro—cations are considerably more potent oxidants than their neutral parent molecules. A solvent medium such as SO_2ClF, which exhibits no known fluoride ion donor properties and has proven its utility as a low-temperature NMR solvent in the study of various ionic fluoride systems and a number of neutral xenon(II) complexes, however, exhibits strongly basic properties toward cationic species, readily reducing all of the known monoxenon cations. Fluorosulfuric acid, on the other hand, is only vigorously attacked by the higher oxidation states of xenon, e.g., XeO_2F^+, $XeOF_3^+$, and XeF_3^+.

With the exception of XeF_5^+, all of the monoxenon cations behave as fluoride acceptors toward fluoride solvents such as HF and BrF_5, giving rise to rapid chemical exchange of fluoride ion in all but the most acidic media. Thus, the simple cations XeF_3^+, $XeOF_3^+$, and XeO_2F^+ have been studied exclusively in SbF_5 solvent owing to their strong oxidizing and fluoride-acceptor properties. In contrast, XeF^+ and XeF_5^+ are readily amenable to study in both SbF_5 and HSO_3F solvents as well as in mixtures of these solvents. Both dixenon cations, $(FXe)_2SO_3F^+$ and $Xe_2F_3^+$, dissociate and/or undergo further reactions in HSO_3F, HF, and SbF_5 solvents but form very stable solutions in BrF_5 which are nonlabile on the NMR time scale near the freezing point of the solvent.

Where solubilities and resistance of the solvent medium to oxidation allow, neutral xenon species have been studied in a variety of solvents of widely varying polarities. In the case of HSO_3F, however, further reactions with the solutes XeF_2, XeF_6, and $FXeMOF_4$ (M = Mo or W) occur giving rise to the corresponding fluorosulfate species **1** and HF. The fluorosulfates $F_5Xe^+SO_3F^-$, $FXeSO_3F$, and $Xe(SO_3F)_2$ have been studied previously in solution by ^{19}F NMR while the species **1** represent a new class of fluorosulfate-bridged xenon(II) compound.

General Trends among ^{129}Xe Chemical Shifts. Using Ramsey's theory of magnetic screening,[17] useful approximations have been developed which make it somewhat easier to interpret NMR shifts of heavy nuclei in compounds of widely ranging geometries. One such approximation takes advantage of cancellation of long-range diamagnetic and paramagnetic contributions to the shielding of the nucleus and represents the shielding of a nucleus such as xenon by the local terms σ_d^{Xe} and σ_p^{Xe}, which are calculated by Ramsey's theory applied only to the electrons on xenon.[18] For xenon, which has a large range of chemical shifts, σ^{Xe-B} from circulation on other atoms B (O or F) is deemed to be relatively small and is neglected, and chemical shift relationships are ascribed solely to variations of σ_p^{Xe}. Using this approach, Jameson and Gutowsky have formulated explicit expressions for the paramagnetic contribution σ_p to the nuclear shielding which include d as well as p orbitals on the atoms in question. These workers subsequently demonstrated the ^{129}Xe chemical shifts could be computed with some success in the limited number of neutral species then known. Their treatment of the problem demonstrated that a localized description of the bonding which employs d hybridization provides a more satisfactory description than a delocalized model without d hybridization. A comparison of their theoretical values for σ_p^{Xe} with our experimental values is given in Table I.

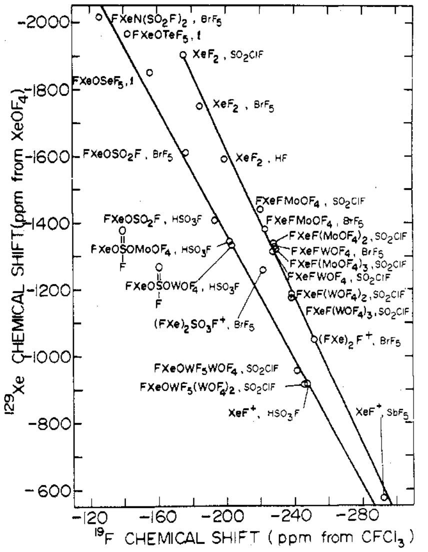

Figure 3. Empirical plot of the ^{129}Xe chemical shift vs. the ^{19}F chemical shift of the terminal fluorine on xenon for some xenon(II) species containing F bridges (lower line) and O bridges (upper line).

From Table II it can be seen that the paramagnetic contribution to the ^{129}Xe chemical shift is extremely large, with chemical shifts ranging from −5331 ppm for $Xe(n\text{-}C_6F_{14})$ to +2077 ppm for XeO_6^{4-}. The large range of chemical shifts for ^{129}Xe is readily anticipated in view of existing trends among other nuclei. A survey of the existing experimental data reveals that the range of chemical shifts not only increases with atomic number Z for a particular period but also increases with Z for a particular group.[19,21] Their periodic dependence places xenon (Z = 54) in a category among nuclei having one of the greatest ranges of NMR chemical shifts observed to date.

It is clear that changes in the ionic character of the xenon–ligand bond will influence the orbital angular momentum of xenon, which, in turn, will affect the magnitude of the paramagnetic term. It may be argued that any increase in the effective electronegativity of xenon, including the removal of fluoride ion, will cause the ionic character of the remaining bonds to decrease and the paramagnetic contribution to the shielding to increase. This should result in shifts to low field. Although the observed deshielding of xenon in the series XeF^+, XeF_3^+, $XeOF_3^+$, and XeO_2F^+ when compared with the chemical shifts of the parent fluorides (Table II) might be correlated with the changes in symmetry about the ^{129}Xe nucleus and resultant changes in the mixing of orbitals, the clear trend of increasing chemical shift with increasing oxidation state of the xenon cannot be ignored. The magnitudes

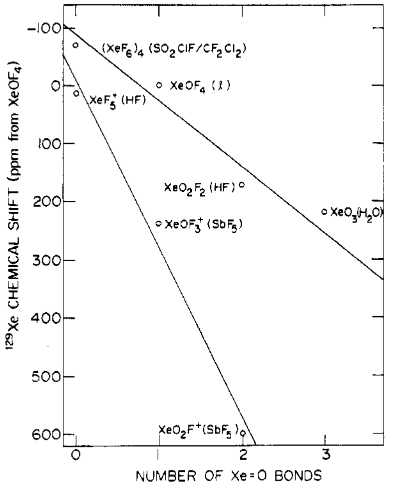

Figure 4. Empirical plot of the number of Xe=O bonds vs. the ^{129}Xe chemical shift for some xenon(VI) species.

of the changes in each step are sufficient to warrant some considerable reliance on the relationship.

Although the ^{129}Xe chemical shifts of xenon(II) compounds occur, as might be anticipated, at much higher field than either xenon(IV) or xenon(VI) species, the rather similar low-field positions of XeF_4 and XeF_3^+ relative to xenon(VI) species are, however, in marked contrast to the corresponding ^{19}F chemical shifts which decrease in the series Xe(VI) > Xe(IV) > Xe(II).[3-7] It is, however, of interest to note that the trend observed for the majority of ^{129}Xe chemical shifts, i.e., Xe(II) < Xe(VI) < Xe(VII), is in agreement with the trend computed by Jameson and Gutowsky for $XeF_2 < XeF_6 < XeOF_4 < XeF_4$ (Table I). Moreover, the observed trend in ^{129}Xe chemical shifts for the series XeF^+, XeF_3^+, and XeF_5^+ in SbF_5 solvent is not consistent with the popular three-center four-electron bond model of the bonding in these species.[22,23] This model leads to the following charge distributions for these cations (dashed lines denote three-center four-electron bonds):

$^{+}Xe{-}F$

II

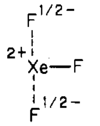

$$\overset{F^{1/2-}}{\vdots}\;{}^{2+}Xe{-}F\;\underset{F^{1/2-}}{\vdots}$$

III

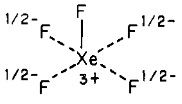

IV

It is reasonable to expect that, with increasing positive charge on the xenon, the contribution to the paramagnetic shielding term would decrease along the series $XeF_5^+ > XeF_3^+ > XeF^+$. In fact, the ^{129}Xe resonance of XeF_5^+ occurs at −600 ppm to high field of XeF_3^+ and at 550 ppm to low field of XeF^+. Although there may be some increase in the charge on xenon in the series XeF^+, XeF_3^+, and XeF_5^+, it is clear that it cannot be nearly so large as this theory proposes. The effect of this charge must be more than compensated by other factors of which the most important perhaps is the increased filling of the valence shell of xenon in going from XeF^+ (four electron pairs) to XeF_3^+ (five electron pairs) to XeF_5^+ (six electron pairs). Thus, xenon(VI) and xenon(IV) chemical shifts are found to be rather similar and, in fact, XeF_5^+ is found to occur at significantly higher field than XeF_3^+.

In general, we note that oxygen is capable of stabilizing the higher oxidation states of xenon; i.e., XeO_3, XeO_4, and XeO_6^{4-} are known, but XeO, XeO_2 and XeF_8 are not. The reason for this is not entirely clear, but steric crowding of bonding pairs of electrons in the valence shell of xenon may be an important factor in the case of XeF_8. From the observed ^{129}Xe chemical shift data (Figure 4), however, it can be inferred that contributions from valence-bond structures of the form $Xe{=}O \leftrightarrow {}^{+}Xe{-}O^{-}$ and ${}^{+}Xe{=}O \leftrightarrow {}^{2+}Xe{-}O^{-}$ are important in stabilizing oxygen-containing species of xenon(VI). Thus, in the two series $(XeF_6)_4$, $XeOF_4$, XeO_2F_2, XeO_3 and XeF_5^+, $XeOF_3^+$, XeO_2F^+ we observe a monotonic deshielding of the central xenon atom with increasing oxygen substitution. While variations of chemical shifts for neutral species may be reasonably ascribed to effects of different solvents, it was possible to observe the cations in a common solvent, SbF_5. Geometrical changes may also contribute to the observed trends in both series. In general, increasing oxygen substitution in both series would lead to a greater degree of p-orbital participation at the expense of d-orbital participation in the bonding. Accordingly, using qualitative arguments based on Jameson and Gutowsky's theory[19,20] the magnitude of d-orbital contributions to σ_p^{Xe} is seen to be substantially less than p-orbital contributions. The paramagnetic term should therefore become more negative, resulting in the observed low-field shifts with increasing oxygen substitution.

Ionic Character of the Xe–F Bond in Xenon(II) Compounds. Although gross geometrical changes occur over series of Xe(IV) and Xe(VI) species, obscuring any attempt at detailed correlations between the ionic character of the xenon–ligand bond and σ_p^{Xe}, similar objections do not arise when series of Xe(II) compounds containing terminal Xe–F groups are chosen. This class of compounds is ideally suited with the linear F–Xe–F(O) geometry being preserved over the entire series of xenon(II) compounds.

When considering the ionic character of the *terminal* Xe–F bond in xenon(II) species, the Xe–F group is regarded as being bridged either to a fluorine, as in XeF_2 and $Xe_2F_3^+$, or to an oxygen, as in $FXeSO_3F$ and $(FXe)_2SO_3F^+$. In the specific case of XeF^+, the cation is not regarded as a totally free cation, but bridged to a solvent fluorine or oxygen atom even though this bridge is labile on the NMR time scale and possibly extensively dissociated.

Upon ionization of XeF_2 to yield XeF^+, the ^{129}Xe chemical shift decreases (Table II). The observed change in the ^{129}Xe chemical shift is in accord with the shielding change predicted by the valence-bond structures XeF^+ (ca. bond order 1) and $F^{-+}Xe{-}F$, $F{-}Xe^{+}F^{-}$ (ca. bond order $^1/_2$). The $Xe_2F_3^+$ cation, which can be represented in terms of the contributing valence-bond structures $F{-}Xe{-}F^{+}Xe{-}F$, $F{-}Xe^{+}F{-}Xe{-}F$, and $F{-}Xe^{+}F^{-+}Xe{-}F$ (plus those for XeF_2) would be expected to possess a terminal Xe–F bond order and a corresponding ^{129}Xe chemical shift roughly intermediate between those of XeF_2 and XeF^+. From Table II, it is clear that this is indeed the case.

Previous studies reveal that there is a near-linear correlation between the ^{19}F chemical shift and ^{129}Xe–^{19}F coupling constant of xenon-containing species.[3,4] For xenon(II) species in particular, the variation in ^{19}F NMR parameters has been related to the ionic character of the Xe–F chemical shifts; chemical shifts have been shown to *increase* with *increasing* ionic character of the terminal Xe–F bond. This is consistent with valence bond structures Va and b where the bonding

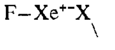

$F{-}Xe^{+-}X\backslash$

Va

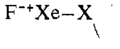

$F^{-+}Xe{-}X\backslash$

Vb

electron pair of the terminal Xe–F bond becomes increasingly more localized with increasing ionic character of the Xe–X (X = F or O) bridge bond.

It is interesting that the semiempirical approach used by Hindman and Svirmickas[14] and by Jameson and Gutowsky[20] for deriving Xe–F bond ionicities from ^{19}F shielding data for XeF_2, XeF_4, XeF_6, and $XeOF_4$ gives trends in ionic character for both series of Xe(II)–F bonds which are opposite to the anticipated trends. Simple valence-bond considerations predict, as we have already noted, covalent bond orders ranging from

$^1/_2$ for XeF_2 to 1 for XeF^+. Using their approach, we have computed ionic characters of terminal Xe–F bonds for XeF_2 in HF (0.69), $Xe_2F_3^+$ in BrF_5 (0.67), and XeF^+ in SbF_5 (0.80). It is clear that ionic characters calculated by this method are opposite to those trends inferred from vibrational spectroscopic and x-ray crystallographic studies,[23] as well as those deduced from the present NMR study.

In the present study, plots of the ^{129}Xe chemical shift vs. the ^{19}F chemical shift of the terminal fluorine on xenon have been shown to exhibit linear relationships over the entire series of xenon(II) species studied (Figure 3). It is clear from Figure 3 that chemical shifts of Xe–F groups form two rather distinct series. In general, the paramagnetic contributions to the ^{129}Xe and ^{19}F chemical shifts of Xe–F groups bonded to oxygen are larger than those of Xe–F groups bonded to fluorine owing to the increased covalent character of the Xe–O bond (and resultant orbital mixing) as opposed to the Xe···F bridge bond. Within each series the covalency of the terminal Xe–F bond is seen to increase with decreasing ^{129}Xe chemical shift and increasing ^{19}F chemical shift. From Figure 3 it can be seen that both lines converge, as expected, in the vicinity of the XeF^+ cation which, in SbF_5 solution, can be regarded as being only very weakly fluorine-bridged to the $Sb_nF_{5n+1}^-$ polyanion, approximating to a free cation.

Within series of closely related compounds in a common solvent the ^{129}Xe resonance serves as a sensitive probe for accessing the relative fluoride-acceptor strengths of a fluorine-bridged ligand. In the case of the species $F—Xe—F\cdots MOF_4(MOF_4)_n$ (n = 0–2, M = Mo or W), which have been recently characterized by ^{19}F NMR spectroscopy,[7,25] the ^{129}Xe resonance in SO_2ClF solvent increases with increasing chain length, in accord with the anticipated fluoride-ion donor strength of the corresponding $[FMOF_4(MOF_4)_n]^-$ anion (Table II). It can also be inferred that the relative acceptor strength rapidly attenuates with increasing chain length. For the oxygen-bridged species, $F–Xe–WOF_5(WOF_4)_n$ (n = 0 or 1), the analogous trend in ligand base strength is evident (Table II). The ^{129}Xe chemical shift trends are fully corroborated by the ^{19}F chemical shifts of the terminal fluorines on xenon, which display the opposite chemical shift trends (ref 25 and Figure 3). It is also of interest to note that the ^{129}Xe chemical shift order, $(WOF_4)_{n+1} > (MoOF_4)_{n+1}$ for a given value of n, is in accord with the greater fluoride-ion acceptor strengths anticipated for the tungsten species. Based on the observed order of ^{129}Xe chemical shifts, the relative order of fluoride-acceptor strengths is $(WOF_4)_3 > (WOF_4)_2 > WOF_4 > (MoOF_4)_3 > (MoOF_4)_2 > MoOF_4$.

Solvation and Temperature Effects. It has been noted in a previous study[3] that the ^{19}F chemical shifts of XeF^+ in SbF_5 and in HSO_3F solvents differ considerably. In the present study, the ^{129}Xe chemical shift of XeF^+ is also shown to be particularly sensitive to solvent composition. The variation of the ^{129}Xe chemical shift of XeF^+ in HSO_3F/SbF_5 solvent mixtures has been studied over the whole composition range. As in the case of the ^{19}F chemical shift, there is a continuous change in the ^{129}Xe chemical shift of XeF^+ from that observed in HSO_3F to that in SbF_5 solvent (Table III). It is clear in both studies that the XeF^+ cation interacts rather strongly with the solvent medium. The interaction presumably occurs by formation of a single additional bridge bond with the strongest electron-pair donor available, i.e., a solvent oxygen of fluorine. In the case of $XeF^+Sb_2F_{11}^-$ in fluorosulfuric acid solvent, the following equilibria are presumed to be important:[5]

$$XeF^+ + 2HSO_3F \rightleftharpoons FXeSO_3F + H_2SO_3F^+ \quad (1)$$

$$XeF^+ + FXeSO_3F \rightleftharpoons (FXe)_2SO_3F^+ \quad (2)$$

As the concentration of SbF_5 is increased, the fluorosulfate species are presumably replaced by the anions $Sb_2F_{11}^-$ and $SbF_5SO_3F^-$ which are, in turn, replaced by the more weakly basic polymeric anions $Sb_nF_{5n+1}^-$. As the XeF^+ cation becomes more weakly bonded to the less basic accompanying anions, the terminal Xe–F bond order increases and its ^{129}Xe chemical shift increases.

Table III. Variation of ^{129}Xe Chemical Shift and ^{129}Xe–^{19}F Coupling Constant for the XeF^+ and XeF_5^+ Ions with Solvent Composition[a]

$[XeF^+]$, m	T, °C	Mole ratio SbF_5:HSO_3F	^{129}Xe chem shift, ppm	$J_{^{129}Xe-^{19}F}$, Hz
0.709	25	SbF_5	−574	7207
1.39	25	SbF_5	−547	7214
0.546	25	8.26	−632	7177
0.546	−10	8.26	−604	7159
0.372	25	4.00	−649	7130
0.372	−10	4.00	−640	7145
0.609	25	2.37	−776	6971
0.609	−10	2.37	−765	6975
0.603	−55	1.48	−882	6808
0.695	−55	1.00	−903	6804
0.716	−70	0	−911	6703

$[XeF_5^+]$, m	T, °C	Mole ratio SbF_5:HSO_3F	^{129}Xe chem shift, ppm	$J_{^{129}Xe-^{19}F}$, Hz
0.108	25	SbF_5	131.8	1507 145
0.444	25	SbF_5	131.8	1528 148
0.187	25	2.17	131.9	1524 154
0.113	25	1.27	131.6	1529 154

[a] Data given are for the solutes $XeF^+Sb_2F_{11}^-$ and $XeF_5^+Sb_2F_{11}^-$.

The chemical shift of XeF^+ in SbF_5–HSO_3F mixtures is also temperature dependent (Table III). The *low*-field shift with decreasing temperature cannot be attributed to shifts in equilibria 1 and 2, favoring $(FXe)_2SO_3F^+$ formation over $FXeSO_3F$. However, further association with the solvent to form $(FXe)_2SO_3F^+$ would be expected to result in a low-field shift with decreasing temperature (cf. chemical shifts of $FXeSO_3F$ and $(FXe)_2SO_3F^+$ in Table II).

Both the ^{19}F and ^{129}Xe chemical shifts have been recorded for XeF_2 in SO_2ClF, BrF_5, and HF solvents at 25 °C. The increase in ^{129}Xe chemical shift and accompanying decrease in ^{19}F chemical shift (Figure 3) with increasing solvent polarity in the series HF > BrF_5 > SO_2ClF suggest that XeF_2 may be solvated through one of its fluorines (structures VIa–c)

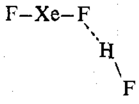

VIa

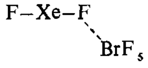

VIb

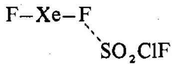

VIc

giving rise to increased XeF^+ character with increasing solvent polarity. The chemical shift of XeF_2 in BrF_5 is also temperature dependent (Table II), increasing with decreasing temperature. This observation is consistent with a higher degree of association between XeF_2 and BrF_5 solvent expected at lower temperatures.

Alternatively, the major contribution to the solvation effect may be viewed in terms of the number of ligands about xenon. It seems evident that the solvation effects for XeF_5^+ and $XeOF_4$ are small when compared to those for XeF^+ and XeF_2 (Tables II and III). Further support is given to this view by a parallel study of XeF_5^+ chemical shifts in SbF_5/HSO_3F mixtures (Table III). The chemical shift of XeF_5^+ is essentially invariant over the complete range of HSO_3F/SbF_5 solvent compositions, while the range observed for XeF^+ is ca. 340 ppm. An increase in the number of substituents around xenon produces a "cage" which more effectively isolates the central xenon atom and/or its lone pair(s) from the solvent. If solvation effects stem from the interaction of the solvent with the lone pairs and/or from weak coordination of the solvent in the xenon valence shell, the solvation effect would be expected to decrease with decreasing numbers of lone pairs (increasing substituents) as we have already noted in the case of XeF_2, XeF^+ and XeF_5, $XeOF_4$.

Ion-pairing effects, which are deemed to be small in relation to solvation effects stemming from covalent interactions of the xenon species with the solvent, do not appear to be important for xenon cations. This is evidenced by the fact that solutions of XeF^+ and XeF_5^+ cations are relatively insensitive to variations in concentration in SbF_5 solution (Table III).

Experimental Section

Materials. The preparation of the solute materials XeF_2,[26] XeF_4,[27] XeF_6,[28] $XeOF_4$,[29] F_5XeSO_3F,[3] $XeF_5^+Sb_2F_{11}^-$,[3] $XeOF_3^+SbF_6^-$,[6] $XeF^+Sb_2F_{11}^-$,[4] $Xe_2F_3^+AsF_6^-$,[4] $FXeSO_3F$,[4] $(FXe)_2SO_3F^+$,[5] $FXeN(SO_2F)_2$,[15] $XeF_2{\cdot}WOF_4$,[7,25] $XeF_2{\cdot}2WOF_4$,[7,25] $XeF_2{\cdot}MoOF_4$,[25] $MoOF_4$,[25] WOF_4,[25] and Na_4XeO_6[30] have all been described elsewhere. XeO_2F_2 was prepared by dissolving stoichiometric amounts of H_2O and XeF_6 in anhydrous HF at room temperature.[6] Solid XeO_2F_2 was isolated by pumping off HF at −78 °C. $XeO_2F^+SbF_6^-$ was prepared by dissolving XeO_2F_2 in HF in a 0.25-in. o.d. FEP reaction tube. Approximately half the stoichiometric amount of SbF_5 was vacuum distilled in. The mixture was rapidly warmed to room temperature to effect solution. Solvent and excess XeO_2F_2 were rapidly pumped off at room temperature to yield solid $XeO_2F^+SbF_6^-$. The purity of the adduct was confirmed by Raman spectroscopy and was shown to contain no detectable amounts of the probable contaminants $XeO_2F^+Sb_2F_{11}^-$,[31] $XeF^+SbF_6^-$,[31] or $XeF^+Sb_2F_{11}^-$.[24]

The purification of the solvents HF, SbF_5, HSO_3F, and BrF_5 has been described elsewhere.[4] CF_2Cl_2 (Matheson) was dried over P_2O_5 for several days prior to use. SO_2ClF was prepared by the interaction of SO_2 and ClF between −78 °C and room temperature and purified by trap to trap distillation.[32] To ensure that no traces of SO_2 were present, SO_2ClF was distilled onto SbF_5 and then distilled onto dry NaF to remove traces of SbF_5 and HF which might be present.

Sample Preparation. All manipulations were carried out under anhydrous conditions on a vacuum line constructed from 316 stainless steel, nickel, Teflon, and FEP.

NMR samples were prepared and vacuum sealed in 10-mm o.d. glass tubes or, in the case of samples containing HF solvent, XeF_6 or $XeOF_4$, in $^3/_8$-in. o.d. FEP tubes attached to Teflon or FEP valves by means of $^1/_4$-in. Teflon nuts and by condensing an appropriate quantity of the solvent into a sample tube containing the solute at −196 °C. Fluorosulfuric acid and SbF_5 samples were prepared in a drybox by syringing the solvent into a sample tube containing the solute cooled to −196 °C. Samples were warmed briefly to −48 °C to effect dissolution, with the exception of those samples utilizing SbF_5 as a solvent; these were warmed to room temperature to effect dissolution. All samples were stored at −196 °C until their spectra could be recorded.

NMR Instrumentation and Methods. Xenon-129 spectra were obtained on natural-abundance compounds using a Bruker HFX-90 spectrometer operating at 22.63 MHz in Fourier-transform mode. A ^{13}C probe with a 10-mm probe insert was used and the magnetic field was adjusted to correspond to the ^{129}Xe resonance frequency. No lock was required as the stability of the instrument was such that over a period of 1 or 2 h no appreciable field drift occurred (i.e., less than ±1 ppm). Liquid $XeOF_4$ at 25 °C was chosen as the external reference for ^{129}Xe. Xenon oxytetrafluoride is readily obtained in high purity and, unlike xenon gas which also suffers from the disadvantage that it exhibits a pressure-sensitive chemical shift, provides a high concentration of ^{129}Xe (4.48 *m*). A dwell time of 23 μs, corresponding to a frequency range of 21.7 kHz, was used. As the ^{129}Xe chemical shift range in the present study is very large (from XeO_6^{4-} to $FXeN(SO_2F)_2$ ca. 4000 ppm), the frequency range (ca. 960 ppm) was not sufficient and it was necessary to vary the spectrometer frequency to obtain the complete range of ^{129}Xe resonances. Referencing was achieved by using intermediate external references whose spectra or fold-back spectra could be compared directly to external $XeOF_4$ or its fold-back spectrum. Interferograms were obtained with 4K points and the Fourier transformation was carried out on 8K or 16K points, depending on the natural line width of the spectrum. With 8K points, the separation between two points in the spectrum was ca. 5 Hz or ca. 0.2 ppm, considerably less than the estimated field drift. The natural line widths of ^{129}Xe transitions were generally small (20 Hz). Most of the spectra were recorded after 4000–8000 scans. Variable temperature studies were carried out using a Bruker temperature controller. Temperatures were measured using a copper–constantan thermocouple inserted directly into the sample region of the probe and were accurate to ±2 °C.

Fluorine-19 NMR spectra were recorded on a JEOL PS-100 spectrometer operating at 94.1 MHz in CW mode using an external deuterium lock in field-sweep mode. Spectra were referenced with respect to external $CFCl_3$ by sample tube interchange.

Acknowledgment. We thank the National Research Council of Canada for the award of an Overseas Postdoctoral Fellowship (G.J.S.), the North Atlantic Treaty Organization for travel grant awards (G.J.S. and J.H.H.), the Science Research Council of Great Britain for operational grant support, and the Universite de Nancy, Nancy, France, for the use of its Fourier-transform NMR facilities.

Registry No. $FXe(SO_2F)_2N$, 53719-78-1; XeF_2, 13709-36-9; $FXeOSO_2F$, 25519-01-1; $Xe(OSO_2F)_2$, 25523-77-7; $FXeOS(O)FOMoOF_4$, 65622-66-4; $FXeOS(O)FOWOF_4$, 65622-65-3; $FXeFWOF_4$, 59433-20-4; $FXeFMoOF_4$, 65622-64-2; $FXeF(MoOF_4)_2$, 65651-37-8; $FXeF(MoOF_4)_3$, 65622-63-1; $FXeF(WOF_4)_2$, 56174-65-3; $FXeF(WOF_4)_3$, 65622-72-2; $FXeOWF_5(WOF_4)$, 65622-71-1; $FXeOWF_5(WOF_4)_2$, 65665-31-8; $FXeOS(O)FOXeF^+$, 48042-49-5; $Xe_2F_3^+$, 37366-73-7; XeF^+, 47936-70-9; $(XeF_6)_4$, 54652-40-3; XeF_5^+, 42879-72-1; $XeOF_4$, 13774-85-1; XeO_2F_2, 13875-06-4; XeO_3, 13776-58-4; $XeOF_3^+$, 44142-97-4; XeF_4, 13709-61-0; XeF_3^+, 42879-71-0; XeO_2F^+, 52078-90-7; XeO_6^{4-}, 29769-62-8; $FXeOTeF_5$, 25599-15-9; $FXeOSeF_5$, 38167-25-8; ^{129}Xe, 13965-99-6.

References and Notes

(1) To whom correspondence should be addressed at the University of Guelph.
(2) (a) Leicester University. (b) University of Guelph. (c) I.U.T. de Rouen. (d) Bruker Spectrospin S.A.
(3) R. J. Gillespie and G. J. Schrobilgen, *Inorg. Chem.*, **13**, 765 (1974).
(4) R. J. Gillespie, A. Netzer, and G. J. Schrobilgen, *Inorg. Chem.*, **13**, 1455 (1974).
(5) R. J. Gillespie and G. J. Schrobilgen, *Inorg. Chem.*, **13**, 1694 (1974).
(6) R. J. Gillespie and G. J. Schrobilgen, *Inorg. Chem.*, **13**, 2370 (1974).
(7) J. H. Holloway, G. J. Schrobilgen, and P. Taylor, *J. Chem. Soc., Chem. Commun.*, 40 (1975).
(8) T. H. Brown, E. B. Whipple, P. H. Verdier, *J. Chem. Phys.*, **38**, 3029 (1963).
(9) T. H. Brown, E. B. Whipple, and P. H. Verdier, "Noble-Gas Compounds", H. H. Hyman, Ed., University of Chicago Press, Chicago, Ill., 1963, p 263.
(10) K. Seppelt and H. H. Rupp, *Z. Anorg. Allg. Chem.*, **409**, 331 (1974).
(11) K. Seppelt and H. H. Rupp, *Z. Anorg. Allg. Chem.*, **409**, 338 (1974).
(12) J. H. Holloway, G. J. Schrobilgen, P. Granger, and C. Brevard, *C. R. Hebd. Seances Acad. Sci.*, **282**, C519 (1976).
(13) H. D. Frame, J. L. Huston, and I. Sheft, *Inorg. Chem.*, **8**, 1549 (1969).
(14) J. C. Hindman and A. Svirmickas, "Noble-Gas Compounds", H. H. Hyman, Ed., University of Chicago Press, Chicago, Ill., 1963, p 251.
(15) R. D. Le Blond and D. D. Des Marteau, *J. Chem. Soc., Chem. Commun.*, 555 (1974).
(16) G. J. Schrobilgen, J. H. Holloway, and P. Granger, to be submitted for publication in *J. Magn. Reson.*
(17) N. F. Ramsey, *Phys. Rev.*, **77**, 576 (1950); **78**, 699 (1950); **83**, 540 (1951); **86**, 243 (1952).
(18) A. Saika and C. P. Slichter, *J. Chem. Phys.*, **22**, 26 (1954).
(19) C. J. Jameson and H. S. Gutowsky, *J. Chem. Phys.*, **40**, 1714 (1964).
(20) C. J. Jameson and H. S. Gutowsky, *J. Chem. Phys.*, **40**, 2285 (1964).
(21) J. Mason, *Adv. Inorg. Chem. Radiochem.*, **18**, 197 (1976).
(22) R. E. Rundle, *J. Am. Chem. Soc.*, **85**, 112 (1963).
(23) D. E. McKee, A. Zalkin, and N. Bartlett, *Inorg. Chem.*, **12**, 1713 (1973).
(24) R. J. Gillespie and B. Landa, *Inorg. Chem.*, **12**, 1383 (1973).
(25) G. J. Schrobilgen and J. H. Holloway, to be submitted for publication in *Inorg. Chem.*
(26) J. L. Weeks and M. S. Matheson in "Inorganic Syntheses", Vol. 8, H. F. Holtzclaw, Ed., McGraw-Hill, New York, N.Y., 1966, p 260.
(27) J. G. Malm and C. L. Chernick, ref 26, p 254.
(28) J. G. Malm and C. F. Chernick, ref 26, p 258.

(29) C. L. Chernick, H. H. Classen, J. G. Malm, and P. L. Plurien in "Noble-Gas Compounds", H. H. Hyman, Ed., University of Chicago Press, Chicago, Ill., 1963, p 106.
(30) E. H. Appelman and J. G. Malm in "Preparative Inorganic Reactions", W. L. Jolly, Ed., Interscience, New York, N.Y., 1965, p 341.
(31) R. J. Gillespie, B. Landa, and G. J. Schrobilgen, *Inorg. Chem.*, **15**, 1256 (1976).
(32) C. L. Schack and R. D. Wilson, *Inorg. Chem.*, **9**, 311 (1970).

Contribution from the Department of Chemistry,
University College, Cardiff, Wales, United Kingdom

Spectroscopic and Magnetic Studies of the 3d Metallocenes

KEVIN R. GORDON and KEITH D. WARREN*

Received April 17, 1977

The electronic spectra of the metallocenes, MCp_2, and 1,1′-dimethylmetallocenes, $M(MeCp)_2$, of the first transition series (M = V, Cr, Mn, Fe, Co, Ni) have been measured between 10 and 50 $cm^{-1} \times 10^3$ in isooctane solution. Assignments are proposed for the d–d and charge-transfer transitions observed, these being based in the latter case largely on the band shifts produced by methyl substitution. For the V, Cr, Mn, and Fe compounds the charge-transfer bands appear to correspond only to ligand → metal excitations ($e_{2u} \rightarrow e_{2g}, a_{1g}, e_{1g}$) but for the Co compounds (and possibly also for Ni) evidence is also found for metal → ligand ($e_{1g} \rightarrow e_{2u}$) transitions. For the V, Cr, Co, and Ni compounds the paramagnetic susceptibilities have been determined in toluene solution by NMR in the temperature range 183–298 K and for the parent compounds also by the Gouy method using solid samples between 83 and 298 K. The V, Cr, and Ni compounds were found to obey the Curie–Weiss law over the ranges studied, but although the V and Ni complexes yielded the spin-only values for the magnetic moment, a substantial orbital contribution was observed for $CrCp_2$ and $Cr(MeCp)_2$. For $Co(MeCp)_2$ the Curie–Weiss law was obeyed over the limited range accessible, although a moment slightly greater than the spin-only value was obtained, and the parent $CoCp_2$ gave a similar moment but deviated markedly from Curie–Weiss behavior.

Introduction

The ligand field model has been shown in recent years to be of great value in the interpretation of the magnetic properties of the d^x configurations of transition-metal sandwich complexes,[1,2] and its utility also extends to the treatment of the d–d and charge-transfer spectra of such systems.[3-6] Nevertheless, although adequate spectroscopic data have previously been reported[7-10] for the d–d bands of VCp_2, $FeCp_2$, and $NiCp_2$, the other neutral metallocene systems of the 3d series have been little studied in this respect, and no systematic attention has been directed toward understanding the nature of the charge-transfer excitations. We therefore now report the results of a study of the solution spectra in isooctane of all neutral 3d metallocenes, together with their 1,1′-dimethyl derivatives, in which both d–d and charge-transfer transitions may be identified; for the latter excitations, of course, it may be deduced whether the bands observed correspond to ligand → metal or metal → ligand transitions, depending upon whether shifts to lower or to higher energies are observed on methyl substitution.

Moreover, numerous magnetic susceptibility measurements have been made on metallocene systems (see ref 6 for a survey), but the data available for $CrCp_2$ and $CoCp_2$, for which orbital contributions to the moment would be expected, are somewhat fragmentary and relate only to a few temperatures, while very few data at all have been reported for the $M(MeCp)_2$ systems. We have therefore measured the susceptibilities down to liquid-nitrogen temperatures of the parent metallocene systems (M = V, Cr, Co, Ni) by the Gouy technique and have made measurements in toluene solution by the NMR method in the upper part of the temperature range. For the very low-melting dimethyl compounds, however, only the latter method proved feasible, thereby restricting the temperature range to 183–298 K. We have not, however, remeasured the susceptibilities of $MnCp_2$ and $Mn(MeCp)_2$ since these compounds have already been extensively investigated,[11,12] and the brown, low-temperature, form of manganocene is in any case now known[13] not to possess a sandwich structure.

Experimental Section

Metallocenes and 1,1′-Dimethylmetallocenes. These were prepared essentially as described by Evans et al.[14] and had properties agreeing with those there reported. All were purified by repeated vacuum sublimation or distillation and gave satisfactory analyses for carbon, hydrogen, and metal. For the chromium compounds the use of anhydrous chromous chloride, rather than chromic chloride, was found to give greatly improved yields; moreover, if $CrCl_3$ is employed, the water-insoluble[15a] rather than the water-soluble[15b] form should be used since the latter affords only negligible yields of the metallocene.

Isooctane (2,2,4-Trimethylpentane). BDH spectroscopic grade isooctane was passed three times through a silica gel column, activated at 300 °C, and distilled onto and from lithium aluminum hydride. It was then vacuum degassed and distilled under pure nitrogen immediately prior to use.

Toluene. Reagent grade material was shaken with concentrated sulfuric acid, care being taken to keep the temperature below 30 °C. The acid layer was then removed and the process repeated until darkening was negligible. The product was then removed by decantation, distilled under pure nitrogen, and finally vacuum degassed and distilled when required.

Spectroscopic Measurements. These were made in a vacuum apparatus containing a silica glass cell, the solvent being manipulated by vacuum distillation and the substrates by vacuum sublimation or distillation. Concentrations were determined by atomic absorption analysis (verified by colorimetric determinations), and Beer's law was established over the range of concentrations used. The optical densities were measured using a Cary 17 spectrophotometer, and diffuse-reflectance measurements were also made on solid samples, using a Beckman DK2A spectroreflectometer with a magnesium oxide reference.

Magnetic Measurements. For solid samples the susceptibilities were measured on a Newport Instruments variable-temperature Gouy balance, and for toluene solutions a modification[16] of the Evans[17] NMR method was adopted, using a Varian 90-MHz instrument. The appropriate corrections for the temperature dependence of the density of toluene were made.

Theory

Spectra. The theoretical basis for the interpretation of the d–d spectra of all d^x configurations in pseudoaxial ($C_{\infty v}$) symmetry has already been described[3-5] and summarized in a recent review.[6] A framework for the understanding of the

0020-1669/78/1317-0987$01.00/0